IIETA International Information and Engineering Technology Association
Advancing the World of Information and Engineering

Mathematical Modelling of Engineering Problems
Vol. 10, No. 6, December, 2023, pp. 1937-1949
Journal homepage: http://iieta.org/journals/mmep

Modelling and Analysis of Vaccination Effects on Hand, Foot, and Mouth Disease Transmission Dynamics

Aakash Mohandoss[1], Gunasundari Chandrasekar[2*], Rashid Jan[3]

[1] Department of Mathematics, College of Engineering and Technology, SRM Institute of Science and Technology, Kattankulathur 603203, Tamil Nadu, India
[2] Department of Mathematics, College of Engineering, Anna University, Chennai 600025, Tamil Nadu, India
[3] Institute of Energy Infrastructure (IEI), Department of Civil Engineering, College of Engineering, University Tenaga Nasional (UNITEN), Putrajaya Campus, Jalan IKRAM-UNITEN, Kajang 43000, Selangor, Malaysia

Corresponding Author Email: gunasundari@annauniv.edu

https://doi.org/10.18280/mmep.100603

Received: 29 June 2023
Revised: 25 August 2023
Accepted: 10 September 2023
Available online: 21 December 2023

Keywords:
dynamical behaviour, hand, foot, and mouth disease vaccination, Numerical results, stability analysis, sensitivity analysis, threshold parameter

ABSTRACT

In this study, the transmission dynamics of hand, foot, and mouth disease (HFMD), incorporating vaccination, were comprehensively assessed. A Susceptible-Vaccinated-Exposed-Infectious-Recovered (SVEIR) model was formulated and its stability was evaluated in relation to disease-free and endemic equilibrium points. The fundamental reproduction number, R_0, was derived utilizing the Next-Generation Matrix method. This work demonstrates the local and global asymptotic stability of both disease-free and endemic equilibria under defined conditions. The local stability of the disease-free equilibrium set was ascertained via the Jacobian matrix method, contingent upon certain prerequisites. Conversely, the stability of the endemic equilibrium set was affirmed using the Routh-Hurwitz criteria. In the context of global stability, a Lyapunov function was employed to establish the disease-free equilibrium case, demonstrating that the equilibrium E_0 is globally asymptotically stable within region Ω. Stability of the endemic equilibrium set for the susceptible and infected compartments was exhibited using Dulac's criteria. Additionally, a sensitivity analysis was performed, revealing a significant correlation of the basic reproduction number to specific parameters, namely A, β_1, β_2, β_3, β_4, and ρ. This analysis indicates that these aforementioned parameters have a substantial influence on HFMD propagation. The analytical findings were corroborated through numerical simulations which further reinforced the validity of the model. This work presents a profound exploration of HFMD transmission dynamics, offering valuable insights for the development of efficacious control strategies.

1. INTRODUCTION

Hand, foot, and mouth disease (HFMD) is a viral infection predominantly affecting children and infants, although adults are not exempt [1]. It commonly manifests on the hands, feet, or mouth, but can occasionally extend to the genitals and buttocks. The incubation period ranges from 2 to 7 days, after which symptoms may present or remain absent [2]. Despite the lack of symptoms in certain individuals, the potential for disease transmission persists.

Common indications of the infection include a mild fever, sore throat, runny nose, cough, fatigue, and loss of appetite, typically lasting for one to two days. Subsequently, tiny uncomfortable blisters may develop, accompanied by small red dots on the toes, soles of the feet, buttocks, and palms [3]. While these sores can cause discomfort, they often resolve with appropriate medication [4].

HFMD, being a viral infection, lacks a specific treatment and often resolves on its own. However, a small subset of children may develop severe central nervous system complications, such as aseptic meningitis, encephalitis, and polio-like paralysis, which can be life-threatening [5].

This pervasive and occasionally fatal disease is primarily attributed to enterovirus 71 (EV71) and coxsackievirus A type 16 (CA16). However, other coxsackievirus strains can also trigger HFMD [6]. The disease is most prevalent in children under seven years old, leading to frequent outbreaks in settings like daycare centers, summer camps, or within families, particularly during the summer and early autumn [7].

Transmission of HFMD is facilitated through contact with infected individuals, interaction with virus-contaminated objects, or the consumption of contaminated food and water. The causative pathogen, EV-71, can survive outside the host under favourable conditions for extended periods. It is noteworthy that while 95% ethanol is the most effective cleaning agent, it does not entirely deactivate EV-71. As such, 75% alcohol-based cleaning products are largely ineffective against the virus, making environmental contamination a significant factor in disease spread.

The first reported case of HFMD was in New Zealand in 1957, followed by its identification in America in 1959 [8]. It has since spread globally, reaching continents such as America

[9], Europe [10], and Asia [11].

A multitude of researchers have explored HFMD transmission using epidemiological models [12, 13]. Mathematical modelling has proven invaluable in managing real-life situations [14-16], particularly with HFMD. Few models, however, incorporate the effects of vaccination. Wang et al. examined the relationship between HFMD outbreaks and meteorological trends in Taiwan and Tokyo, respectively [16]. Chen et al. used a SIR-based dynamic model to explore the disease's transmissibility [17]. Phonchan and Naowarat performed a sensitivity analysis on an SEIQR model [18]. Huang et al. investigated the seasonality of HFMD transmission using an SEIAR model [19]. Shi et al. developed a SVEII$_e$QRW model to assess the impact of the EV71 vaccine on HFMD in China [20]. The model described in reference [1] is a fractional-order SEIR type that considers treatment as a control parameter.

In this study, a SVEIR compartment was considered, assuming that individuals recovering from HFMD become susceptible again, rejoining the susceptible compartment, while others receive the vaccine and join the vaccinated compartment. This assumption guided the formulation of an epidemic model of HFMD incorporating vaccination effects to unravel the complexities of this infection and propose effective control strategies.

The structure of this paper is as follows: Section 2 presents the five-dimensional nonlinear mathematical model, discussing the positivity and boundedness of system (1). Equilibrium and stability analyses are presented in Sections 3 and 4, respectively. Section 5 addresses the sensitivity analysis, while Section 6 focuses on numerical simulations. The paper concludes with a brief summary in Section 8.

2. FORMULATION OF MATHEMATICAL MODEL

In this section, we formulate a five compartment HFMD model, named *SVEIR*. The underlying structure of the model comprises classes of individuals are susceptible $S(t)$, vaccinated $V(t)$, exposed $E(t)$, infected $I(t)$ and recovered $R(t)$. In this we assume that, not all vaccinated individuals are set free from this virus, some have a chance of getting exposed to this virus. We further consider that people who have recovered from HFMD do not possess a lifelong immunity to the illness. Therefore, we believe that recovered persons are susceptible at a rate of α and after recovery some individuals will take vaccine, so they join the vaccinated compartment at the rate of α_1. By considering the above assumptions a simple nonlinear mathematical model is formulated.

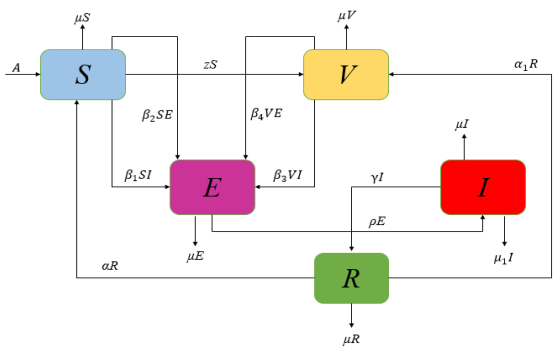

Figure 1. Flow chart of the transmission dynamics of HFMD infection

$$\begin{aligned}
\frac{dS}{dt} &= A - \beta_1 SI - \beta_2 SE - \mu S - zS + \alpha R,\\
\frac{dV}{dt} &= zS - \beta_3 VI - \beta_4 VE - \mu V + \alpha_1 R,\\
\frac{dE}{dt} &= \beta_1 SI + \beta_2 SE + \beta_3 VI + \beta_4 VE - \rho E - \mu E,\\
\frac{dI}{dt} &= \rho E - \gamma I - \mu I - \mu_1 I,\\
\frac{dR}{dt} &= \gamma I - \mu R - \alpha R - \alpha_1 R.
\end{aligned} \tag{1}$$

Further the model (1) is simplified as below:

$$\begin{aligned}
\frac{dS}{dt} &= A - \beta_1 SI - \beta_2 SE - k_1 S + \alpha R,\\
\frac{dV}{dt} &= zS - \beta_3 VI - \beta_4 VE - \mu V + \alpha_1 R,\\
\frac{dE}{dt} &= \beta_1 SI + \beta_2 SE + \beta_3 VI + \beta_4 VE - k_2 E,\\
\frac{dI}{dt} &= \rho E - k_3 I,\\
\frac{dR}{dt} &= \gamma I - k_4 R.
\end{aligned} \tag{2}$$

where,

$$k_1 = \mu + z, k_2 = \rho + \mu, k_3 = \gamma + \mu + \mu_1 \text{ and } k_4 = \mu + \alpha + \alpha_1.$$

Table 1. Description of parameters

Parameter	Description
A	Recruitment rate
β_1	The rate at which S are getting the infection from I
β_2	The rate at which S are getting the infection from E
β_3	Transmission rate from I to V
β_4	Transmission rate from E to V
μ	Natural mortality rate
α_1	Rate from R to V
ρ	Progression rate from E to I
γ	Recovery rate due to treatment
μ_1	Disease related death
α	Rate from R to S
z	Vaccination rate of the population

Here, A denotes the recruitment rate. β_1 and β_2 are the transmission rate at which S are getting the infection from I and E respectively, whereas β_3 and β_4 represents the transmission rate from I to V and E to V respectively. The natural mortality rate and disease related death rate are denoted by μ and μ_1, whereas the recovery rate due to treatment was represented by γ. The progression rate from E to I was given by the parameter ρ. The parameter α and α_1 represents the rate from R to S and V. Finally, the vaccination rate of the population was described by the parameter z. Also, the flow chart of the transmission dynamics of HFMD infection was

displayed in Figure 1 and the parameter description was provided in Table 1.

2.1 Positivity and boundedness

In this, we analyse the positivity and boundedness of the proposed system. It is important to check while building mathematical models because it ensures that, the solutions remain positive and bounded, which enable us in effective validation. If a model's outcomes violate these constraints, it often signals issues with the model's formulation or parameterization. So, it is necessary to check positivity and boundedness for the proposed system.

Theorem 2.1 Solution of the system (1) in R^5 are positive.

Proof. From system (1) we have,

$$\left.\frac{dS}{dt}\right|_{S=0} = A+\alpha R \geq 0,$$
$$\left.\frac{dV}{dt}\right|_{V=0} = zS+\alpha_1 R \geq 0,$$
$$\left.\frac{dE}{dt}\right|_{E=0} = \beta_1 SI+\beta_3 VI \geq 0,$$
$$\left.\frac{dI}{dt}\right|_{I=0} = \rho E \geq 0,$$
$$\left.\frac{dR}{dt}\right|_{R=0} = \gamma I \geq 0.$$

Hence, all the population and parameters are nonnegative. Thus, it is assured that none of the system's (1) solutions are negative. This ends the proof.

Theorem 2.2 Solution of the proposed system (1) in R^5 are bounded in the positive invariant region.

Proof. From the system (1), the total population is $N=S+V+E+I+R$ and the rate of change of whole population is

$$\begin{aligned}\frac{dN}{dt} &= \frac{dS}{dt}+\frac{dV}{dt}+\frac{dE}{dt}+\frac{dI}{dt}+\frac{dR}{dt}\\ &= A-\mu(S+V+E+I+R)-\mu_1 I\\ &= A-\mu N-\mu_1 I.\end{aligned}$$

In the absence of disease, we have $I=0$, therefore $\frac{dN}{dt} = A-\mu N$. This gives that $lim\ sup\ N \leq \frac{A}{\mu}$. Therefore, all of the solutions to the equations S, V, E, I and R are constrained by $\frac{A}{\mu}$. Hence the biologically feasible region of the system (1) is provided by positive invariant set:

$$\Omega = \left\{ \begin{array}{l} (S,V,E,I,R) \in R^5 \,\middle|\, S(t)>0, V(t)\geq 0, \\ E(t)\geq 0, I(t)\geq 0, R(t)\geq 0, S+V+E+I+R \leq \frac{A}{\mu} \end{array} \right\} \quad (3)$$

3. ANALYSIS OF THE MODEL

In this section, we analyse the existence of equilibrium points for the system (2). Here we obtained two equilibrium points namely $E_0 = (S^0, V^0, E^0, I^0, R^0)$ and $E_1 = (S^*, V^*, E^*, I^*, R^*)$.

3.1 Disease free equilibrium points (E_0)

For the system (2), we obtain the disease-free equilibrium points as $E_0 = \left(\frac{A}{k_1}, \frac{zA}{k_1\mu}, 0,0,0\right)$.

3.2 Basic reproduction number (R_0)

The basic reproduction number, represented as R_0, is the number of newly infected people in an uninfected population caused by a single infected individual. The traditional method for determining the expression for R_0 is known as the next-generation matrix method. For this, we consider only the disease compartment from our system (2).

$$\begin{aligned}\frac{dE}{dt} &= \beta_1 SI+\beta_2 SE+\beta_3 VI+\beta_4 VE - k_2 E,\\ \frac{dI}{dt} &= \rho E - k_3 I.\end{aligned}$$

Now by using above equation, we define $F(t), V(t)$.

$$F(t) = \begin{pmatrix} \beta_1 SI+\beta_2 SE+\beta_3 VI+\beta_4 VE \\ 0 \end{pmatrix},\ V(t) = \begin{pmatrix} k_2 E \\ -\rho E + k_3 I \end{pmatrix}$$

The Jacobian of $F(t)$ and $V(t)$ at $\boldsymbol{E_0}$ is obtained and it is denoted as F and V respectively.

$$\mathrm{F} = \begin{pmatrix} \beta_2 S+\beta_4 V & \beta_1 S+\beta_3 V \\ 0 & 0 \end{pmatrix}, \mathrm{V} = \begin{pmatrix} k_2 & 0 \\ -\rho & k_3 \end{pmatrix}$$

Now the matrix FV^{-1} is given by,

$$\mathrm{FV}^{-1} = \begin{pmatrix} \frac{\rho(S\beta_1+V\beta_3)}{k_2 k_3}+\frac{S\beta_2+V\beta_4}{k_2} & \frac{S\beta_1+V\beta_3}{k_3} \\ 0 & 0 \end{pmatrix} \quad (4)$$

The spectral radius of the next generation matrix FV^{-1} determines the R_0 for the system (2). Therefore, we $R_0 = \frac{\rho S\beta_1+\rho V\beta_3+S\beta_2 k_3+k_3 V\beta_4}{k_2 k_3}$. Now, by substituting the disease-free equilibrium point we get,

$$R_0 = \frac{\rho\left(\frac{A}{k_1}\right)\beta_1+\rho\left(\frac{zA}{k_1\mu}\right)\beta_3+\left(\frac{A}{k_1}\right)\beta_2 k_3+k_3\left(\frac{zA}{k_1\mu}\right)\beta_4}{k_2 k_3}. \quad (5)$$

3.3 Endemic equilibrium points (E_0)

For the system (2), we obtain the endemic equilibrium points as $E_1 = (S^*, V^*, E^*, I^*, R^*)$, where,

$$S^* = \frac{\rho A k_4 + \alpha\gamma\rho I^*}{k_4(\rho k_1 + \beta_1\rho I^* + \beta_2 k_3 \rho I^*)},$$

$$E^* = \frac{k_3 I^*}{\rho}, R^* = \frac{\gamma I^*}{k_4},$$

$$V^* = \frac{\rho z k_4 (\frac{\rho A k_4 + \alpha\gamma\rho I^*}{k_4(\rho k_1 + \beta_1\rho I^* + \beta_2 k_3\rho I^*)} + \rho\alpha_1\gamma I^*)}{k_4(\beta_3\rho I^* + \beta_4 k_3 I^* + \rho\mu)},$$

I^* is the root of the below Eq. (6).

$$G(I^*) = M_1 I^{*3} + M_2 I^{*2} + M_3 I^* - M_4 = 0 \quad (6)$$

Here,

$$\begin{aligned}
M_1 &= \rho^4\beta_1\alpha\gamma k_4\beta_3\beta_2 k_3 + \rho^4\beta_1^2\alpha\gamma k_4\beta_3 + \rho^3\beta_1^2\alpha\gamma k_3 k_4\beta_4 + \rho^3\beta_1\alpha\gamma k_4\beta_4 k_3^2\beta_2 \\
&+\rho^2\alpha\gamma\beta_2^2 k_3^3 k_4\beta_4 + \rho^2\alpha\gamma\beta_2 k_3^2\beta_4 k_4\beta_1 + \rho^3\alpha\gamma\beta_2 k_3 k_4\beta_3\beta_1 + \rho^3\alpha\gamma\beta_2 k_3^2 k_4\beta_3\beta_2 \\
&+\rho^4\alpha_1\gamma\beta_1\beta_2 k_3 k_4 + \rho^4\alpha_1\gamma\beta_1^2 k_4 + \rho^4\alpha_1\gamma\beta_2^2 k_3^2 k_4 + \rho^4\alpha_1\gamma\beta_2 k_3 k_4\beta_1 \\
&+\rho^4\alpha\gamma\beta_3 z\beta_2 k_3 k_4 + \rho^3\alpha_1\gamma k_3^2\beta_1\beta_2 k_4 - \rho^2 k_3^2 k_4^2\beta_1^2\beta_4 - \rho^2 k_3^2 k_4^2\beta_1\beta_4\beta_2 \\
&-\rho^3 k_3 k_4^2\beta_1^2\beta_3 - \rho^3 k_3^2 k_4^2\beta_1\beta_2\beta_3 - \rho^2 k_3^3\beta_2 k_4^2\beta_4\beta_1 - \rho^2 k_3^4\beta_2 k_4^2\beta_4\beta_2 \\
&-\rho^3 k_3^2\beta_2 k_4^2\beta_3\beta_1 - \rho^3 k_3^3\beta_2 k_4^2\beta_3\beta_2, \\
M_2 &= \rho^4\beta_1 A k_4^2\beta_3\beta_2 k_3 + \rho^4\beta_1^2 A k_4^2\beta_3 + \rho^3\beta_1^2 A k_4^2\beta_4 k_3 + \rho^3\beta_1 A k_4^2\beta_4 k_3^2\beta_2 \\
&+\rho^4\beta_1^2\alpha\gamma\mu k_4 + \rho^4\beta_1\alpha\gamma\mu k_4\beta_2 k_3 + \rho^4\beta_1\alpha\gamma k_4\beta_3 k_1 + \rho^3\beta_1\alpha\gamma\beta_4 k_3 k_4 k_1 \\
&+\rho^2\beta_2^2 k_3^2 A k_4^2\beta_4 + \rho^3\alpha\gamma\beta_2 k_3\mu k_4\beta_1 + \rho^3\beta_2^2 k_3^2 A k_4^2\beta_3 + \rho^3\beta_2 k_3 A k_4^2\beta_3\beta_1 \\
&+\rho^2\beta_2 k_3^2 A k_4^2\beta_4\beta_1 + \rho^3\alpha\gamma\beta_2^2 k_3^2\mu k_4 + \rho^3\alpha\gamma\beta_2 k_3 k_4\beta_3 k_1 + \rho^2\alpha\gamma\beta_2 k_3^2\beta_4 k_4 k_1 \\
&+\rho^4\alpha_1\gamma\beta_2 k_3 k_4 k_1 + \rho^4\alpha\gamma\beta_1 k_4 k_1 + \rho^4\alpha_1\gamma k_1 k_4\beta_1 + \rho^4\alpha_1\gamma k_1\beta_2 k_3 k_4 \\
&+\rho^2\alpha\gamma\beta_3 z k_4\beta_1 + \rho^3\alpha\gamma\beta_4 z k_3 k_4\beta_1 + \rho^3\alpha\gamma\beta_4 z k_3^2\beta_2 k_4 + \rho^3\alpha_1\gamma k_3\beta_1^2 k_4 \\
&+\rho^3\alpha_1\gamma k_3^2\beta_2^2 k_4 + \rho^3\alpha_1\gamma k_3^2\beta_2 k_4\beta_1 - \rho^2 k_3^2 k_4^2 k_1\beta_4\beta_2 - \rho^3 k_3 k_4^2\beta_1^2\mu \\
&-\rho^3 k_3^2 k_4^2 k_1\beta_3\beta_2 - \rho^3 k_3 k_4^2 k_1\beta_3\beta_1 - \rho^2 k_3^2 k_4^2\beta_4\beta_1 - \rho^3 k_3^2 k_4^2\beta_1\mu\beta_2 \\
&-\rho^3 k_3 k_4^2\beta_1\beta_3 k_1 - \rho^2 k_3 k_4^2\beta_1\beta_4 k_1 - \rho^3 k_3^2\beta_2 k_4^2\mu\beta_2 - \rho^3 k_3^2\beta_2 k_4^2\mu\beta_1 \\
&-\rho^3 k_3^2\beta_2 k_4^2\beta_3 k_1 - \rho^2 k_3^2\beta_2 k_4^2\beta_4 k_1, \\
M_3 &= \rho^4\beta_1 A k_4^2\mu\beta_1 + \rho^4\beta_1 A k_4^2\mu\beta_2 k_3 + \rho^3\beta_1 A k_4^3 k_3 k_1 + \rho^4\beta_1 A k_4^2\beta_3 k_1 \\
&+\rho^4\beta_1\alpha\gamma\mu k_4 k_1 + \rho^3\beta_2 k_3 A k_4^4\mu + \rho^3\beta_2^2 k_3^2 A k_4^2\mu + \rho^3\beta_2 k_3 A k_4^2\beta_3 k_1 \\
&+\rho^2\beta_2 k_3^2 A k_4^2\beta_4 k_1 + \rho^3\alpha\gamma\beta_2 k_3\mu k_4 k_1 + \rho^2\alpha\gamma\beta_3 z k_4 k_1 + \rho^4\alpha_1\gamma k_1^2 k_4 \\
&+\rho^4 A k_4^2\beta_3 z\beta_1 + \rho^4 A k_4^2\beta_3 z\beta_2 k_3 + \rho^3\alpha\gamma\beta_4 z k_3 k_4 k_1 + \rho^3\alpha_1\gamma k_3\beta_1 k_4 k_1 \\
&+\rho^3\alpha_1\gamma k_3^2\beta_2 k_4 k_1 + \rho^3 A k_4^2\beta_4 z k_3\beta_1 + \rho^3 A k_4^2\beta_4 z k_3^2\beta_2 + \rho^3\alpha_1\gamma k_3 k_1 k_4\beta_1 \\
&+\rho^3\alpha_1\gamma k_3^2 k_1\beta_2 k_4 - \rho^3 k_4^2 k_1\mu\beta_1 k_3 - \rho^3 k_4^2 k_1\mu\beta_2 k_3^2 - \rho^3 k_3 k_4^2 k_1^2\beta_3 - \rho^2 k_3^2 k_4^2 k_1^2\beta_4 \\
&-\rho^3 k_3 k_4^2\beta_1\mu k_1 - \rho^3 k_3^2 k_4^2\beta_2\mu k_1, \\
M_4 &= \rho^4\beta_1 A k_4^2 k_1\mu + \rho^3\beta_2 k_3 A k_4^2\mu k_1 + \rho^4 A k_4^2\beta_3 z k_1 + \rho^3 A k_4^2\beta_4 z k_3 k_1 \\
&+\rho^3\alpha_1\gamma k_3 k_1^2 k_4 - \rho^3\mu k_1^2 k_4^2 k_3.
\end{aligned}$$

where,

$$\begin{aligned}
M_1 > 0 \text{ if } & \rho^4\beta_1\alpha\gamma k_4\beta_3\beta_2 k_3 + \rho^4\beta_1^2\alpha\gamma k_4\beta_3 > \rho^2 k_3^2 k_4^2\beta_1^2\beta_4 + \rho^2 k_3^2 k_4^2\beta_1\beta_4\beta_2 \\
&+\rho^3 k_3 k_4^2\beta_1^2\beta_3 + \rho^3 k_3^2 k_4^2\beta_1\beta_2\beta_3 + \rho^2 k_3^3\beta_2 k_4^2\beta_4\beta_1 + \rho^2 k_3^4\beta_2 k_4^2\beta_4\beta_2 \\
&+\rho^3 k_3^2\beta_2 k_4^2\beta_3\beta_1 + \rho^3 k_3^3\beta_2 k_4^2\beta_3\beta_2 \\
M_2 > 0 \text{ if } & \rho^4\beta_1 A k_4^2\beta_3\beta_2 k_3 + \rho^4\beta_1^2 A k_4^2\beta_3 + \rho^3\beta_1^2 A k_4^2\beta_4 k_3 > \rho^2 k_3^3 k_4^2 k_1\beta_4\beta_2 \\
&+\rho^3 k_3 k_4^2\beta_1^2\mu + \rho^3 k_3^2 k_4^2 k_1\beta_3\beta_2 + \rho^3 k_3 k_4^2 k_1\beta_3\beta_1 + \rho^2 k_3^2 k_4^2\beta_4\beta_1 \\
&+\rho^3 k_3^2 k_4^2\beta_1\mu\beta_2 + \rho^3 k_3 k_4^2\beta_1\beta_3 k_1 + \rho^2 k_3 k_4^2\beta_1\beta_4 k_1 + \rho^3 k_3^2\beta_2 k_4^2\mu\beta_2 \\
&+\rho^3 k_3^2\beta_2 k_4^2\mu\beta_1 + \rho^3 k_3^2\beta_2 k_4^2\beta_3 k_1 + \rho^2 k_3^2\beta_2 k_4^2\beta_4 k_1 \\
M_3 > 0 \text{ if } & \rho^4\beta_1 A k_4^2\mu\beta_1 + \rho^4\beta_1 A k_4^2\mu\beta_2 k_3 > \rho^3 k_4^2 k_1\mu\beta_1 k_3 + \rho^3 k_4^2 k_1\mu\beta_2 k_3^2 \\
&+\rho^3 k_3 k_4^2 k_1^2\beta_3 + \rho^2 k_3^2 k_4^2 k_1^2\beta_4 + \rho^3 k_3 k_4^2\beta_1\mu k_1 + \rho^3 k_3^2 k_4^2\beta_2\mu k_1 \\
M_4 < 0 \text{ if } & \rho^4\beta_1 A k_4^2 k_1\mu + \rho^3\beta_2 k_3 A k_4^2\mu k_1 + \rho^4 A k_4^2\beta_3 z k_1 + \rho^3 A k_4^2\beta_4 z k_3 k_1 \\
&+\rho^3\alpha_1\gamma k_3 k_1^2 k_4 < \rho^3\mu k_1^2 k_4^2 k_3
\end{aligned}$$

Therefore, $G(I^*) = M_1 I^{*3} + M_2 I^{*2} + M_3 I^* - M_4 = 0$. Now, clearly, we can comment that $M_1, M_2, M_3 > 0$ and $M_4 < 0$ Here we apply Descartes' rule of signs. Since this is used to find the number of possible positive roots. So, by using Descartes rule of signs, we can able to find the positive roots, which was displayed in Table 2.

Table 2. Existence of positive roots

Coefficients	Signs of Coefficients	No of Sign Change	No of Possible Positive Roots
M_1	Positive	0	No root
M_2	Positive	0	No root
M_3	Positive	0	No root
M_4	Negative	1	Unique root

4. STABILITY ANALYSIS OF THE MODEL

In this section we show the local and global stability analysis of disease-free equilibrium and endemic equilibrium points. The Jacobian matrix for our system (2) is given by:

$$J = \begin{pmatrix} -\beta_1 I - \beta_2 E - k_1 & 0 & -\beta_2 S & -\beta_1 S & \alpha \\ z & -\beta_3 I - \beta_4 E - \mu & -\beta_4 V & -\beta_3 V & \alpha_1 \\ \beta_1 I + \beta_2 E & \beta_3 I + \beta_4 E & \beta_2 S + \beta_4 V - k_2 & \beta_3 V + \beta_1 S & 0 \\ 0 & 0 & \rho & -k_3 & 0 \\ 0 & 0 & 0 & \gamma & -k_4 \end{pmatrix} \quad (7)$$

4.1 Local stability analysis

Theorem 4.1 When $R_0 < 1, E_0 = (S^0, V^0, E^0, I^0, R^0)$ is locally asymptotically stable.

Proof. For the system (2), the Jacobi matrix at disease free equilibrium E_0 is obtained as follows,

$$J_0 = \begin{pmatrix} -k_1 & 0 & -\frac{\beta_2 A}{k_1} & -\frac{\beta_1 A}{k_1} & \alpha \\ z & -\mu & -\frac{\beta_4 z A}{k_1\mu} & -\frac{\beta_3 z A}{k_1\mu} & \alpha_1 \\ 0 & 0 & \frac{\beta_2 A}{k_1} + \frac{\beta_4 z A}{k_1\mu} - k_2 & \frac{\beta_3 z A}{k_1\mu} + \frac{\beta_1 A}{k_1} & 0 \\ 0 & 0 & \rho & -k_3 & 0 \\ 0 & 0 & 0 & \gamma & -k_4 \end{pmatrix} \quad (8)$$

Clearly, from the above matrix we can say, $-\mu, -k_1, -k_4$ are the three eigen values. Here λ_1 and λ_2 can be computed from the below matrix as shown in Table 3.

$$\begin{pmatrix} \frac{\beta_2 A}{k_1} + \frac{\beta_4 z A}{k_1\mu} - k_2 & \frac{\beta_3 z A}{k_1\mu} + \frac{\beta_1 A}{k_1} \\ \rho & -k_3 \end{pmatrix} \quad (9)$$

They are $\lambda_1 = x_1 + \sqrt{x_2 + x_3}$ and $\lambda_2 = x_1 - \sqrt{x_2 + x_3}$, where,

$$x_1 = A\beta_2\mu - k_1k_2\mu - k_1k_3\mu + A\beta_4 z,$$

$$x_2 = A^2\beta_2^2\mu^2 + k_1^2k_2^2\mu^2 + 2k_1^2k_2k_3\mu^2 + k_1^2k_3^2\mu^2 + 2A^2\beta_2\beta_4\mu z + A^2\beta_4^2 z^2$$
$$-2A\beta_2k_1k_2\mu^2 - 2A\beta_2k_1k_3\mu^2 - 2A\beta_4k_1k_2\mu z - 2A\beta_4k_1k_3\mu z,$$

$$x_3 = 4(A\beta_2k_1k_3\mu^2 + \beta_1Ak_1\rho\mu^2 + A\beta_4k_1k_3\mu z + A\beta_3k_1\rho\mu z - k_1^2k_2k_3\mu^2).$$

Table 3. Necessary conditions to be stable

Eigen Value	Sign	Conditions	Stability
λ_1	Negative	$x_1 < 0, x_2 > 0$ $x_3 > 0$ and hence $x_1 > \sqrt{x_2 + x_3}$	Asymptotically Stable
λ_2	Negative	$x_1 < 0, x_2 > 0$ $x_3 > 0$ and hence $x_1 - \sqrt{x_2 + x_3} < 0$	Asymptotically Stable

Clearly, all the five eigen values are negative with the above conditions. Hence our DFE, $E_0 = (S^0, V^0, E^0, I^0, R^0)$ is locally asymptotically stable, which was presented graphically in Figure 2.

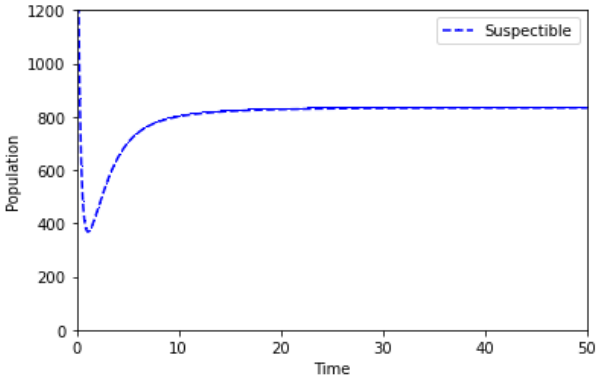

(a)

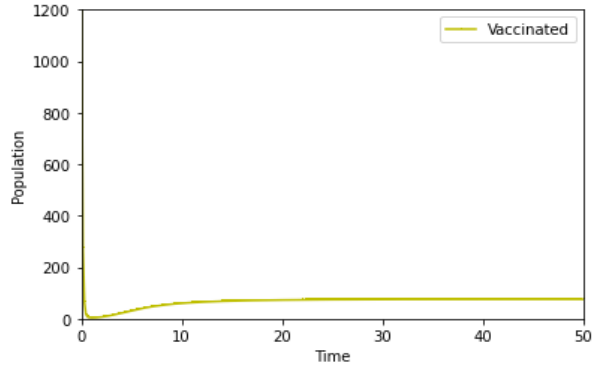

(b)

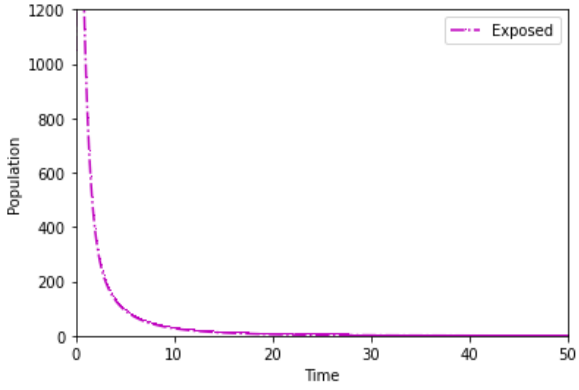

(c)

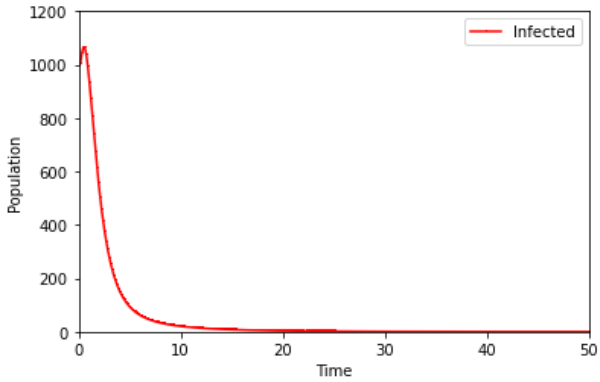

(d)

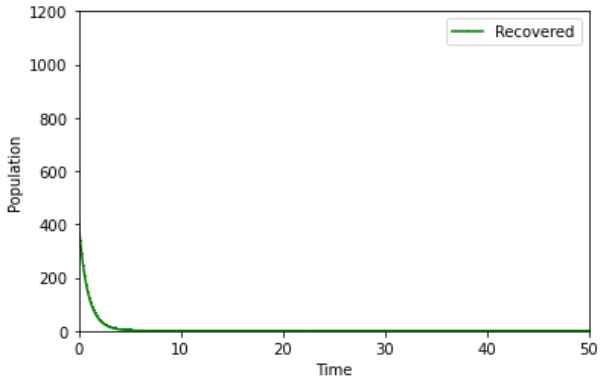

(e)

Figure 2. Variation of (a) Susceptible population with time, (b) Vaccinated population with time, (c) Exposed population with time, (d) Infected population with time and (e) Recovered population with time for $R_0 < 1$

Theorem 4.2 $E_1 = (S^*, V^*, E^*, I^*, R^*)$ is locally asymptotically stable whenever it satisfies the below conditions, otherwise it is said to be unstable.

(i) $y_i > 0$, where $i = 1, 2, 3, 4, 5$,

(ii) $y_1y_2y_3 > y_3^2 + y_1^2y_4$,

(iii) $(y_1y_4 - y_5)(y_1y_2y_3 - y_3^2 - y_1^2y_4) > y_5(y_1y_2 - y_3)^2 + y_1y_5^2$.

Proof. For the system (2), the Jacobi matrix at endemic equilibrium E_1 is obtained as follows,

$$J_1 = \begin{pmatrix} -\beta_1I^* - \beta_2E^* - k_1 & 0 & -\beta_2S^* & -\beta_1S^* & \alpha \\ z & -\beta_3I^* - \beta_4E^* - \mu & -\beta_4V^* & -\beta_3V^* & \alpha_1 \\ \beta_1I^* + \beta_2E^* & \beta_3I^* + \beta_4E^* & \beta_2S^* + \beta_4V^* - k_2 & \beta_3V^* + \beta_1S^* & 0 \\ 0 & 0 & \rho & -k_3 & 0 \\ 0 & 0 & 0 & \gamma & -k_4 \end{pmatrix} \quad (10)$$

Let us consider,

$$a_{11} = -\beta_1I^* - \beta_2E^* - k_1,\ a_{13} = -\beta_2S^*,\ a_{14} = -\beta_1S^*,\ a_{15} = \alpha,\ a_{21} = z,$$
$$a_{22} = -\beta_3I^* - \beta_4E^* - \mu,\ a_{23} = -\beta_4V^*,\ a_{24} = -\beta_3V^*,\ a_{25} = \alpha_1,$$
$$a_{31} = \beta_1I^* + \beta_2E^*,\ a_{32} = \beta_3I^* + \beta_4E^*,\ a_{33} = \beta_2S^* + \beta_4V^* - k_2,$$
$$a_{34} = \beta_3V^* + \beta_1S^*, a_{43} = \rho,\ a_{44} = -k_3, a_{54} = \gamma,\ a_{55} = -k_4.$$

Now, the characteristic equation of the J_1 matrix is,

$$\Rightarrow \Lambda^5 + y_1\Lambda^4 + y_2\Lambda^3 + y_3\Lambda^2 + y_4\Lambda + y_5 = 0, \quad (11)$$

where,

$$y_1 = -a_{11} - a_{22} - a_{33} - a_{44} - a_{55},$$

$$y_2 = a_{44}a_{55} + a_{33}a_{55} + a_{22}a_{55} + a_{11}a_{55} + a_{33}a_{44} + a_{22}a_{44} + a_{11}a_{44} + a_{22}a_{33} + a_{11}a_{33} + a_{11}a_{22} - a_{34}a_{43} - a_{23}a_{32} - a_{13}a_{31},$$

$$y_3 = a_{34}a_{43}a_{55} + a_{23}a_{32}a_{55} + a_{13}a_{31}a_{55} + a_{23}a_{32}a_{44} + a_{13}a_{31}a_{44} + a_{22}a_{34}a_{43} + a_{11}a_{34}a_{43} + a_{11}a_{23}a_{32} + a_{13}a_{22}a_{31} - a_{33}a_{44}a_{55} - a_{22}a_{44}a_{55} - a_{11}a_{44}a_{55} - a_{22}a_{33}a_{55} - a_{11}a_{33}a_{55} - a_{11}a_{22}a_{55} - a_{22}a_{33}a_{44} - a_{11}a_{33}a_{44} - a_{11}a_{22}a_{44} - a_{24}a_{32}a_{43} - a_{14}a_{31}a_{43} - a_{11}a_{22}a_{33} - a_{13}a_{21}a_{32},$$

$$y_4 = a_{22}a_{33}a_{44}a_{55} + a_{11}a_{33}a_{44}a_{55} + a_{11}a_{22}a_{44}a_{55} + a_{24}a_{32}a_{43}a_{55} + a_{14}a_{31}a_{43}a_{55} + a_{11}a_{22}a_{33}a_{55} + a_{13}a_{21}a_{32}a_{55} + a_{11}a_{22}a_{33}a_{44} + a_{11}a_{23}a_{32}a_{44} + a_{13}a_{21}a_{32}a_{44} + a_{11}a_{24}a_{32}a_{43} + a_{14}a_{22}a_{31}a_{43} - a_{23}a_{32}a_{44}a_{55} - a_{13}a_{31}a_{44}a_{55} - a_{22}a_{34}a_{43}a_{55} - a_{11}a_{34}a_{43}a_{55} - a_{11}a_{23}a_{32}a_{55} - a_{13}a_{22}a_{31}a_{55} - a_{25}a_{32}a_{43}a_{54} - a_{15}a_{31}a_{43}a_{54} - a_{13}a_{22}a_{31}a_{44} - a_{1}a_{22}a_{34}a_{43} - a_{14}a_{21}a_{32}a_{43},$$

$$y_5 = a_{11}a_{23}a_{32}a_{44}a_{55} + a_{13}a_{22}a_{31}a_{44}a_{55} + a_{11}a_{22}a_{34}a_{43}a_{55} + a_{14}a_{21}a_{32}a_{43}a_{55} + a_{11}a_{25}a_{32}a_{43}a_{54} + a_{15}a_{22}a_{31}a_{43}a_{54} - a_{11}a_{22}a_{33}a_{44}a_{55} - a_{13}a_{21}a_{32}a_{44}a_{55} - a_{11}a_{24}a_{32}a_{43}a_{55} - a_{14}a_{22}a_{31}a_{43}a_{55} - a_{15}a_{21}a_{32}a_{43}a_{54}.$$

Now we use Routh-Hurwitz criteria, since it is a powerful analytical tool used in mathematical modelling, particularly in the study of dynamic systems. This helps us to determine stability and oscillatory behaviour of systems, providing insights that are crucial for understanding the behaviour of various systems. So by Routh Hurwitz criteria, E_1 is locally asymptotically stable if $y_i > 0$, where $i = 1, 2, 3, 4, 5$, $y_1y_2y_3 > y_3^2 + y_1^2y_4$, $(y_1y_4 - y_5)(y_1y_2y_3 - y_3^2 - y_1^2y_4) > y_5(y_1y_2 - y_3)^2 + y_1y_5^2$. For our case we get,

$$y_1 > 0, if\ a_{11} + a_{22} + a_{33} + a_{44} + a_{55} < 0,$$

$$y_2 > 0, if\ a_{11}a_{33} + a_{11}a_{22} > a_{34}a_{43} + a_{23}a_{32} + a_{13}a_{31},$$

$$y_3 > 0, if\ a_{11}a_{34}a_{43} + a_{11}a_{23}a_{32} + a_{13}a_{22}a_{31} > a_{33}a_{44}a_{55} + a_{22}a_{44}a_{55} + a_{11}a_{44}a_{55} + a_{22}a_{33}a_{55} + a_{11}a_{33}a_{55} + a_{11}a_{22}a_{55} + a_{22}a_{33}a_{44} + a_{11}a_{33}a_{44} + a_{11}a_{22}a_{44} + a_{24}a_{32}a_{43} + a_{14}a_{31}a_{43} + a_{11}a_{22}a_{33} + a_{13}a_{21}a_{32},$$

$$y_4 > 0, if\ a_{11}a_{24}a_{32}a_{43} + a_{14}a_{22}a_{31}a_{43} > a_{23}a_{32}a_{44}a_{55} + a_{13}a_{31}a_{44}a_{55} + a_{22}a_{34}a_{43}a_{55} + a_{11}a_{34}a_{43}a_{55} + a_{11}a_{23}a_{32}a_{55} + a_{13}a_{22}a_{31}a_{55} + a_{25}a_{32}a_{43}a_{54} + a_{15}a_{31}a_{43}a_{54} + a_{13}a_{22}a_{31}a_{44} + a_{1}a_{22}a_{34}a_{43} + a_{14}a_{21}a_{32}a_{43},$$

$$y_5 > 0, if\ a_{11}a_{23}a_{32}a_{44}a_{55} > a_{11}a_{22}a_{33}a_{44}a_{55} + a_{13}a_{21}a_{32}a_{44}a_{55} + a_{11}a_{24}a_{32}a_{43}a_{55} + a_{14}a_{22}a_{31}a_{43}a_{55} + a_{15}a_{21}a_{32}a_{43}a_{54}.$$

According to the Routh-Hurwitz criteria theorem, we obtain that all the roots of the characteristic equation have negative real parts. Hence EE, $E_1 = (S^*, V^*, E^*, I^*, R^*)$ is locally asymptotically stable, which was presented graphically in Figure 3.

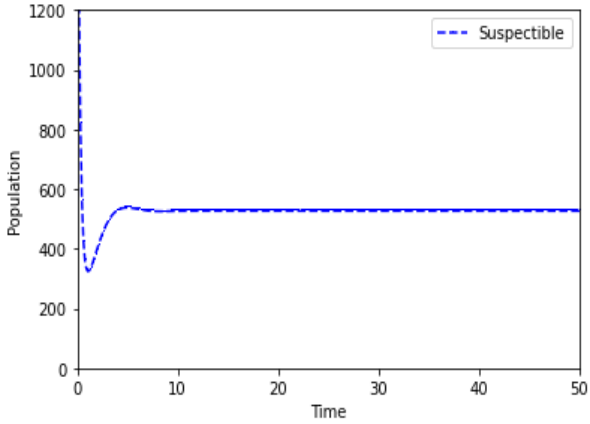

(a)

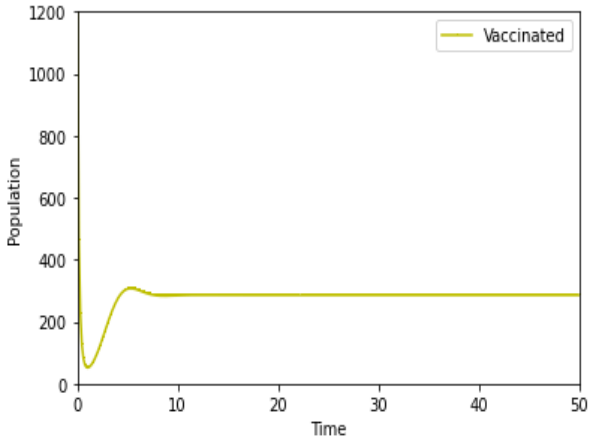

(b)

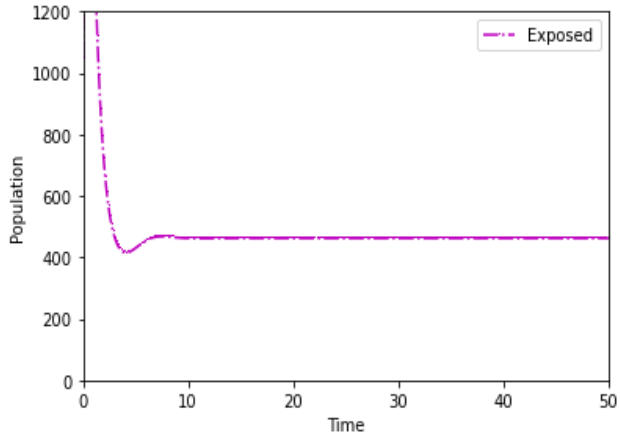

(c)

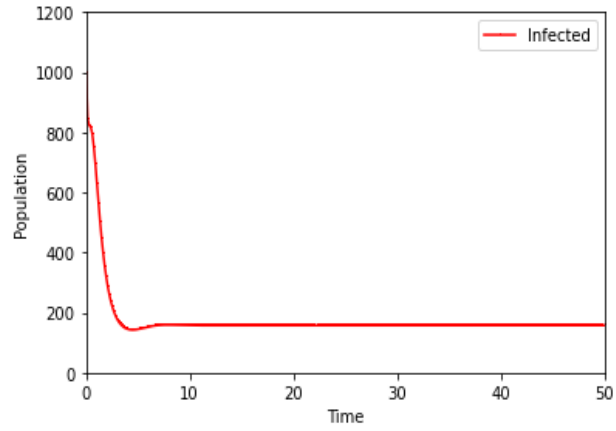

(d)

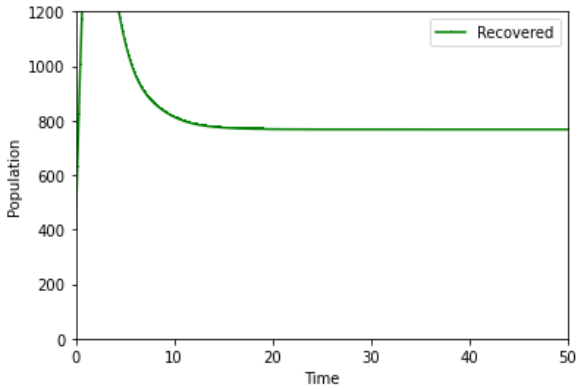

(e)

Figure 3. Variation of (a) Susceptible population with time, (b) Vaccinated population with time, (c) Exposed population with time, (d) Infected population with time and (e) Recovered population with time for $R_0 > 1$

4.2 Global stability analysis

Theorem 4.3 When $R_0 < 1$, E_0 of the system (2) is globally asymptotically stable.

Proof. A Lyapunov function is a mathematical construct used in stability analysis to assess the stability properties of a dynamic system, such as a differential equation or a difference equation. Specifically, it helps to determine whether the system's equilibrium points are stable, asymptotically stable, or unstable. So, here, we construct the Lyapunov function.

$$V_1 = \frac{1}{k_2 k_3} E + \frac{A\beta_2}{\rho k_1 k_2 k_3} I \tag{12}$$

Differentiating the above equation, we get,

$$\dot{V}_1 = \frac{1}{k_2 k_3} \dot{E} + \frac{A\beta_2}{\rho k_1 k_2 k_3} \dot{I} \tag{13}$$

$$\dot{V}_1 = \frac{1}{k_2 k_3}(\beta_1 SI + \beta_2 SE + \beta_3 VI + \beta_4 VE - k_2 E) + \frac{A\beta_2}{\rho k_1 k_2 k_3}(\rho E - k_3 I)$$

We know that, $S \le \frac{A}{k_1}$, $V \le \frac{zA}{k_1 \mu}$, $E \le 0$, $R \le 0$ and hence Eq. (13) becomes

$$\dot{V}_1 = \frac{1}{k_2 k_3}\left(\beta_1 \frac{A}{k_1} I + \beta_3 \frac{zA}{k_1 \mu} I\right) + \frac{A\beta_2}{\rho k_1 k_2 k_3}(-k_3 I)$$

By simplifying we get,

$$\dot{V}_1 = \frac{I}{\rho}\left[\frac{(A\rho\beta_1\mu + A\beta_3 z\rho + Az\beta_4 k_3 + A\mu k_3\beta_2) - 2A\mu k_3 k_2 - Az\beta_4 k_3}{k_1 k_2 k_3 \mu}\right]$$

$$\le \frac{I}{\rho}[R_0 - m], \text{where } m = \frac{Az\beta_4 k_3 - 2A\mu k_3 k_2}{k_1 k_2 k_3 \mu}$$

Clearly, for $I = 0$, we get $\dot{V}_1 = 0$ and $\dot{V}_1 \le 0$ if and only if $R_0 < 1$. From Lasalle's Invariance Principle, we can say that every solution of the system (2) with initial condition in Ω approaches E_0 as t tends to infinity. Since we already know region Ω is positively invariant, which was described in Eq. (3). Hence E_0 is globally asymptotically stable in Ω whenever R_0 is less than one. Hence the proof.

Theorem 4.4 The endemic equilibrium E_1 is globally stable in the region Ω.

Proof. Here we prove the global stability of the region Ω, so we choose S and I compartments and omit the V, E, R population. Then in the positive quadrant of the S, I plane we apply Dulac's criteria with multiplier $D = \frac{1}{I}$. We consider,

$$F_1 = A - \beta_1 SI - \mu S - zS,$$
$$F_2 = -\gamma I - \mu I - \mu_1 I$$

By applying Dulac's criteria,

$$DF_1 = \frac{A}{I} - \beta_1 S - \frac{\mu S}{I} - \frac{zS}{I},$$
$$DF_2 = -\gamma - \mu - \mu_1$$

Now partial differentiating DF_1 and DF_2 with respect to S and I, we get,

$$\frac{\partial(DF_1)}{\partial S} = \frac{\partial}{\partial S}\left(\frac{A}{I} - \beta_1 S - \frac{\mu S}{I} - \frac{zS}{I}\right),$$
$$= -\beta_1 - \frac{\mu}{I} - \frac{z}{I},$$
$$\frac{\partial(DF_2)}{\partial I} = \frac{\partial}{\partial I}(-\gamma - \mu - \mu_1) = 0$$

Here, $\frac{\partial(DF_1)}{\partial S} + \frac{\partial(DF_2)}{\partial I} = -\frac{\beta_1}{I} - \frac{\mu}{I} - \frac{z}{I} < 0$

We can conclude from the above-mentioned condition that the region Ω does not contain any periodic solution. Also, whenever t tends to infinity, every solution starting in the positive quadrant of the SI plane with $I>0$ and $S + I \le \frac{A}{\mu}$ approaches (S^*, I^*). Therefore, the remaining compartments in the system (1) shows $V \to V^*$, $E \to E^*$ and $R \to R^*$. Hence $(S^*, V^*, E^*, I^*, R^*)$ is globally stable in the region Ω.

5. SENSITIVITY ANALYSIS

The sensitivity analysis assists in identifying the various causes of change in the model's input parameters that can be attributed to model's output variation. This can be used to determine the importance of each parameter in the spread of the disease. As a result, it is necessary to identify the parameters that have a significant influence on the basic reproduction number R_0. The normalised forward sensitivity index is the ratio of the relative change in the variable to the relative change in this key parameter. If the result is positive, it means that an increase in the value of the parameter leads to an increase in the value of R_0. But if the sensitivity index is negative, it means that the parameter and R_0 are not related in the same way.

Definition 5.1 The normalized forward sensitivity index of R_0 that depends differentiably on a parameter p is defined by $\Theta_p = \frac{\partial R_0}{\partial p}.\frac{p}{R_0}$, where, R_0 is the basic reproduction number and p is the parameter.

Preposition 5.1 The explicit expression of R_0 is given by,

$$R_0 = \frac{\rho\left(\frac{A}{k_1}\right)\beta_1 + \rho\left(\frac{zA}{k_1\mu}\right)\beta_3 + \left(\frac{A}{k_1}\right)\beta_2 k_3 + k_3\left(\frac{zA}{k_1\mu}\right)\beta_4}{k_2 k_3}$$

The R_0 is influenced by several parameters. So, we can derive analytical expressions for its sensitivity to each of these parameters by computing the normalised forward sensitivity index, which is calculated as follows:

Proof. From the above Definition 5.1, we describe the sensitivity of basic reproduction number as follows. Here,

$$\frac{\partial R_0}{\partial A}.\frac{A}{R_0} = 1,$$

$$\frac{\partial R_0}{\partial \beta_1}.\frac{\beta_1}{R_0} = \frac{\beta_1\rho\mu}{\beta_1\rho\mu + \beta_2\mu(\mu+\gamma+\mu_1) + \beta_3\rho z + \beta_4(\mu+\mu_1+\gamma)z} > 0,$$

$$\frac{\partial R_0}{\partial \beta_2}.\frac{\beta_2}{R_0} = \frac{\beta_2\mu(\mu+\gamma+\mu_1)}{\beta_1\rho\mu + \beta_2\mu(\mu+\gamma+\mu_1) + \beta_3\rho z + \beta_4(\mu+\mu_1+\gamma)z} > 0,$$

$$\frac{\partial R_0}{\partial \beta_3}.\frac{\beta_3}{R_0} = \frac{\beta_3\rho z}{\beta_1\rho\mu + \beta_2\mu(\mu+\gamma+\mu_1) + \beta_3\rho z + \beta_4(\mu+\mu_1+\gamma)z} > 0,$$

$$\frac{\partial R_0}{\partial \beta_4}.\frac{\beta_4}{R_0} = \frac{\beta_4(\mu+\gamma+\mu_1)z}{\beta_1\rho\mu + \beta_2\mu(\mu+\gamma+\mu_1) + \beta_3\rho z + \beta_4(\mu+\mu_1+\gamma)z} > 0,$$

$$\frac{\partial R_0}{\partial \gamma}.\frac{\gamma}{R_0} = -\frac{\rho\gamma(\beta_1\mu+\beta_3 z)}{(\mu+\gamma+\mu_1)(\beta_1\rho\mu + \beta_2\mu(\mu+\gamma+\mu_1) + \beta_3\rho z + \beta_4(\mu+\gamma+\mu_1)z)} < 0,$$

$$\frac{\partial R_0}{\partial \mu_1}.\frac{\mu_1}{R_0} = -\frac{\rho\mu_1(\beta_1\mu+\beta_3 z)}{(\mu+\gamma+\mu_1)(\beta_1\rho\mu + \beta_2\mu(\mu+\gamma+\mu_1) + \beta_3\rho z + \beta_4(\mu+\gamma+\mu_1)z)} < 0,$$

$$\frac{\partial R_0}{\partial \mu}.\frac{\mu}{R_0} = \frac{\mu(\beta_1\rho + \beta_2(2\mu+\gamma+\mu_1) + \beta_4 z)}{\beta_1\mu\rho + \beta_2\mu(\mu+\gamma+\mu_1) + \beta_3\rho z + \beta_4(\mu+\gamma+\mu_1)z} - \frac{\rho(3\mu^2 + (\gamma+\mu_1)z + 3\mu(\gamma+\mu_1+z))}{(\rho+\mu)(\mu+\gamma+\mu_1)(\mu+z)},$$

$$\frac{\partial R_0}{\partial \rho}.\frac{\rho}{R_0} = \frac{\rho(\beta_1\mu^2 - \beta_2\mu(\mu+\gamma+\mu_1) + \beta_3\mu z - \beta_4(\mu+\gamma+\mu_1)z)}{(\rho+\mu)(\beta_1\rho\mu + \beta_2\mu(\mu+\gamma+\mu_1) + \beta_3\rho z + \beta_4(\mu+\gamma+\mu_1)z)},$$

$$\frac{\partial R_0}{\partial z}.\frac{z}{R_0} = \frac{-\mu z\begin{pmatrix}\beta_1\rho(\rho(\mu+\gamma+\mu_1)+\mu(\mu+\mu_1+\mu\mu_1)) - \beta_3\rho(\mu^2+\rho(\mu+\gamma+\mu_1)\\ +\gamma z + \mu(\gamma+\mu_1-\mu_1 z)) + (\mu+\gamma+\mu_1)(\beta_2(\rho(\mu+\gamma+\mu_1)+\mu(\mu+\mu_1+\mu\mu_1))\\ -\beta_4(\mu^2+\rho(\mu+\gamma+\mu_1)+\gamma z+\mu(\gamma+\mu_1-\mu_1 z)))\end{pmatrix}}{(\rho+\mu)(\mu+\gamma+\mu_1)(\mu+z)(\beta_1\rho\mu + \beta_2\mu(\mu+\gamma+\mu_1) + \beta_3\rho z + \beta_4(\mu+\gamma+\mu_1)z)}$$

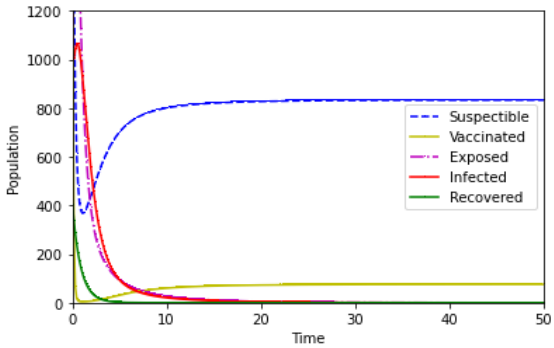

(a)

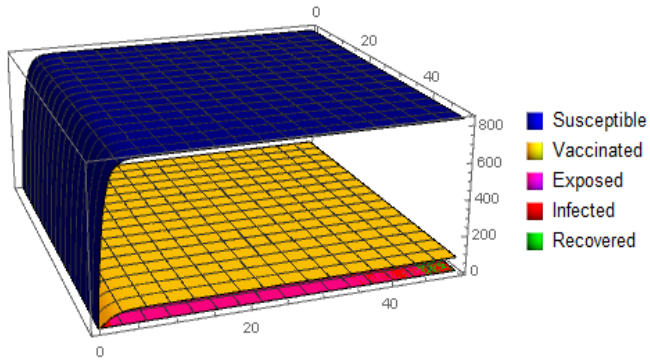

(b)

Figure 4. (a) Stability of the disease free equilibrium point when $R_0 < 1$ and (b) Three dimensional view of stability at DFE E_0

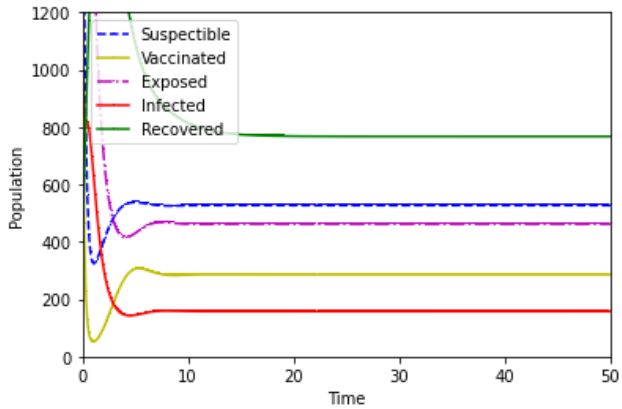

(a)

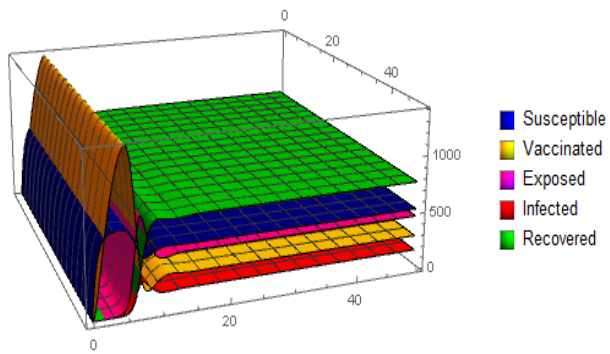

(b)

Figure 5. (a) Stability of the endemic equilibrium point when $R_0 > 1$ and (b) Three dimensional view of stability at EE E_1

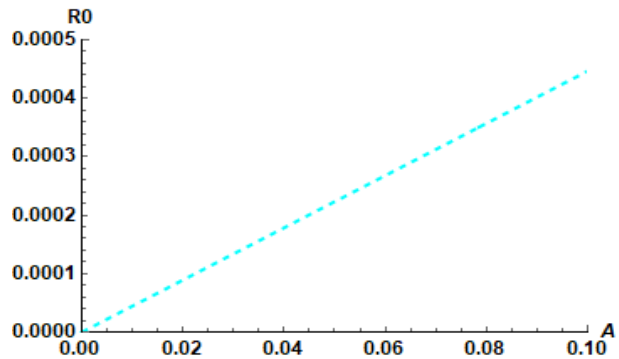

(a)

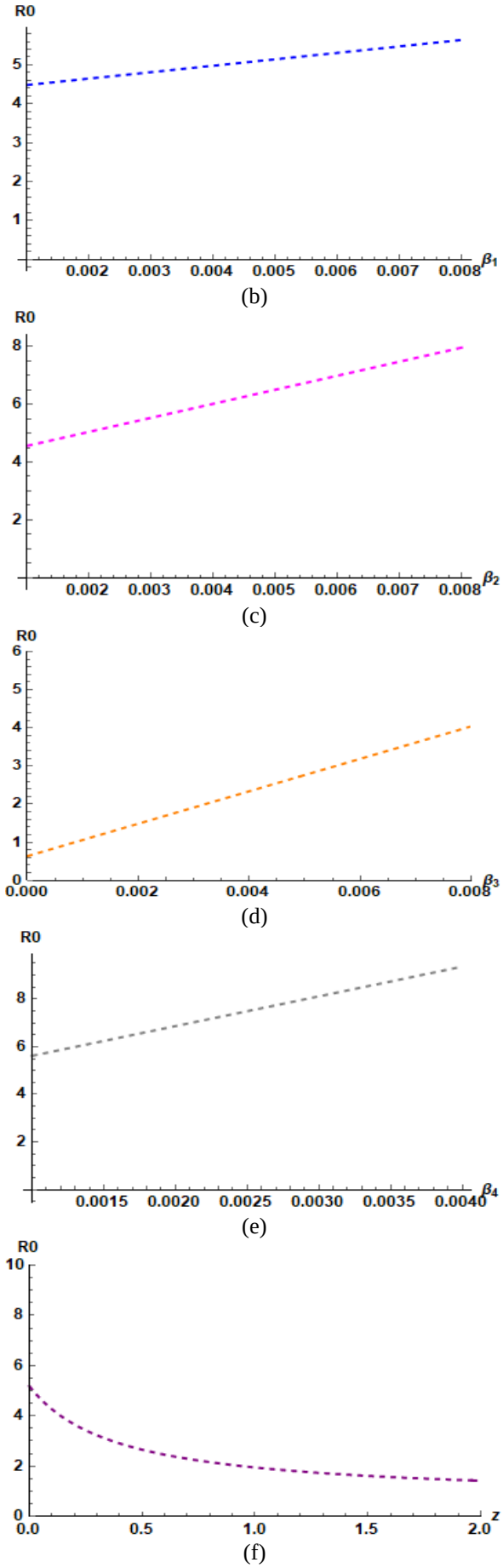

Figure 6. (a) R_0 with (a) the variation of A, (b) the variation of β_1, (c) the variation of β_2, (d) the variation of β_3, (e) the variation of β_4 and (f) the variation of z

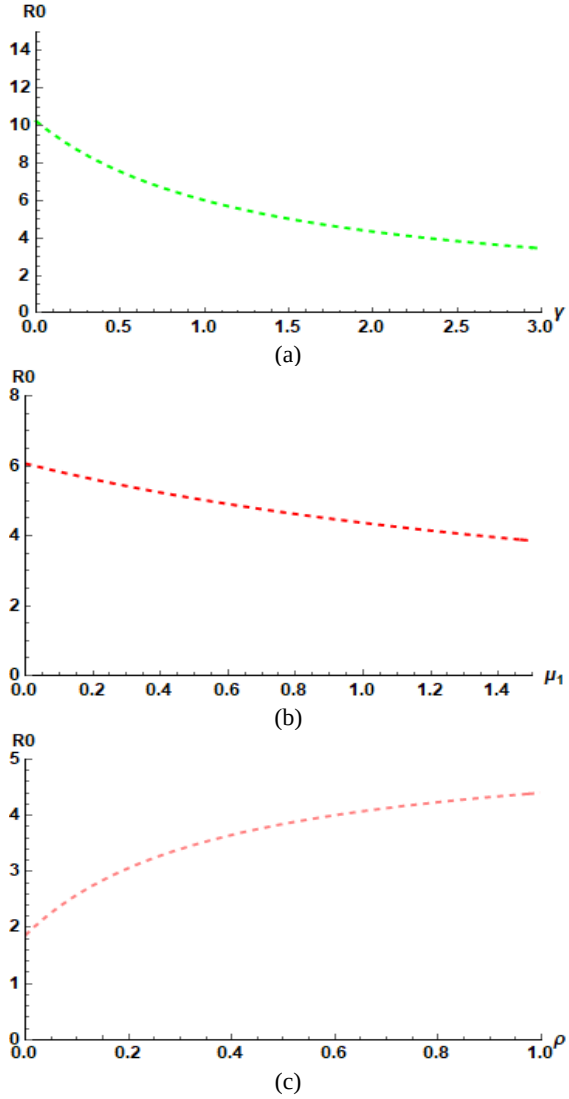

Figure 7. R_0 with (a) the variation of γ, (b) the variation of μ_1 and (c) the variation of ρ

Table 4. Sensitivity of basic reproduction number for the parameter

Parameter	Sensitivity Index of R_0	Sign
A	$\frac{\partial R_0}{\partial A}\cdot\frac{A}{R_0}$	Positive
β_1	$\frac{\partial R_0}{\partial \beta_1}\cdot\frac{\beta_1}{R_0}$	Positive
β_2	$\frac{\partial R_0}{\partial \beta_2}\cdot\frac{\beta_2}{R_0}$	Positive
β_3	$\frac{\partial R_0}{\partial \beta_3}\cdot\frac{\beta_3}{R_0}$	Positive
β_4	$\frac{\partial R_0}{\partial \beta_4}\cdot\frac{\beta_4}{R_0}$	Positive
z	$\frac{\partial R_0}{\partial z}\cdot\frac{z}{R_0}$	-
γ	$\frac{\partial R_0}{\partial \gamma}\cdot\frac{\gamma}{R_0}$	Negative
μ_1	$\frac{\partial R_0}{\partial \mu_1}\cdot\frac{\mu_1}{R_0}$	Negative
μ	$\frac{\partial R_0}{\partial \mu}\cdot\frac{\mu}{R_0}$	-
ρ	$\frac{\partial R_0}{\partial \rho}\cdot\frac{\rho}{R_0}$	-

From the above Table 4, we note that the parameters A, β_1, β_2, β_3 and β_4 are non negative. Hence an increase in the value of these parameters leads to an increase in the value of basic reproduction R_0 and also, we observe the parameters γ and μ_1 are not positive. Therefore, a drop in the value of the basic

reproduction number R_0 follows an increase in the value of these parameters. Due to the complexity of obtained equations, here it is tedious to find the signs and dependency of R_0 for the parameters of z, μ and ρ.

6. NUMERICAL RESULTS

In this section, we perform some numerical simulations to show the dynamics of the proposed system (1) in order to support our mathematical arguments. We assume different set of parameter values to simulate our system (1) for disease free equilibrium. Let us consider: A=1000, β_1=0.0009, β_2=0.0008, β_3=0.009, β_4=0.00008, μ=0.9, μ_1=0.0422, z=0.0999, α=0.05, α_1=0.005, γ=0.005 and ρ=0.7. For this set of parameter values, we obtain

$$R_0 = \frac{\rho\left(\frac{A}{k_1}\right)\beta_1 + \rho\left(\frac{zA}{k_1\mu}\right)\beta_3 + \left(\frac{A}{k_1}\right)\beta_2 k_3 + k_3\left(\frac{zA}{k_1\mu}\right)\beta_4}{k_2 k_3}$$

$$= 0.9448 < 1$$

Therefore, our basic reproduction number R_0 corresponding to disease free equilibrium set is less than one. Hence our DFE $E_0 = (S^0, V^0, E^0, I^0, R^0)$ is stable, which is demonstrated in the Figure 4(a) and (b). Now, we made few changes in the parameter value to simulate the system (1) for endemic equilibrium. For this, we consider: μ =0.3888, μ_1 =0.92, z=0.999, α =0.0005, α_1 =0.0005, γ =0.9005 and ρ=0.9005. For this set of parameter values, we obtain

$$R_0 = \frac{\rho\left(\frac{A}{k_1}\right)\beta_1 + \rho\left(\frac{zA}{k_1\mu}\right)\beta_3 + \left(\frac{A}{k_1}\right)\beta_2 k_3 + k_3\left(\frac{zA}{k_1\mu}\right)\beta_4}{k_2 k_3}$$

$$= 1.7371 > 1$$

Therefore, our basic reproduction number R_0 corresponding to endemic equilibrium set is greater than one. Hence the EE, $E_1 = (S^*, V^*, E^*, I^*, R^*)$ is stable, which is demonstrated in the Figure 5(a) and (b). By using the above mentioned parametric values, we have calculated the sensitivity index value, which was described in Table 5.

Table 5. Calculated sensitivity index

Parameter	Sensitivity Index of R_0	Calculated Sensitivity Index
A	$\frac{\partial R_0}{\partial A}\cdot\frac{A}{R_0}$	1
β_1	$\frac{\partial R_0}{\partial \beta_1}\cdot\frac{\beta_1}{R_0}$	0.0333622
β_2	$\frac{\partial R_0}{\partial \beta_2}\cdot\frac{\beta_2}{R_0}$	0.0870484
β_3	$\frac{\partial R_0}{\partial \beta_3}\cdot\frac{\beta_3}{R_0}$	0.857223
β_4	$\frac{\partial R_0}{\partial \beta_4}\cdot\frac{\beta_4}{R_0}$	0.0223666
z	$\frac{\partial R_0}{\partial z}\cdot\frac{z}{R_0}$	-0.128233
γ	$\frac{\partial R_0}{\partial \gamma}\cdot\frac{\gamma}{R_0}$	-0.527391
μ_1	$\frac{\partial R_0}{\partial \mu_1}\cdot\frac{\mu_1}{R_0}$	-0.255301
μ	$\frac{\partial R_0}{\partial \mu}\cdot\frac{\mu}{R_0}$	-1.52996
ρ	$\frac{\partial R_0}{\partial \rho}\cdot\frac{\rho}{R_0}$	0.15291

Here in Figures 6 and 7, the sensitivity index of each parameter that are associated with R_0 are presented graphically. Each figure shows the effect of our parameter with R_0 on the transmission of HFMD. Figure 6 (a), (b), (c), (d), (e) and Figure 7 (c) shows that, increasing the value of A, $\beta_1, \beta_2, \beta_3, \beta_4, \rho$ raises the chances of the population to be infected with HFMD. Therefore, these increasing transmission rate spreads the HFMD with time. Also, these rates contribute equally to the spread of infection. So, from this we conclude that increasing the value of $A, \beta_1, \beta_2, \beta_3, \beta_4, \rho$ increases the basic reproduction number i.e., these parameters directly proportional to basic reproduction number R_0.

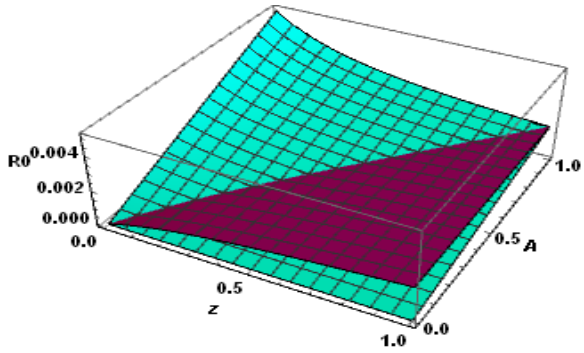

(a)

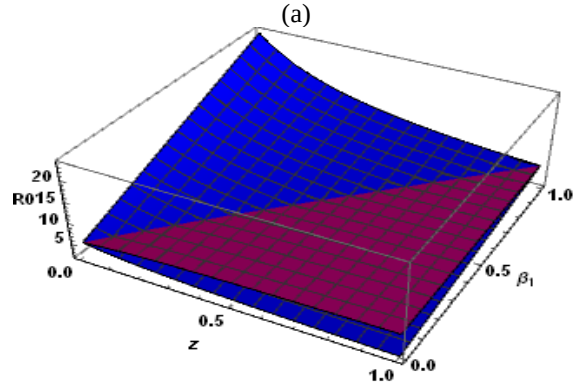

(b)

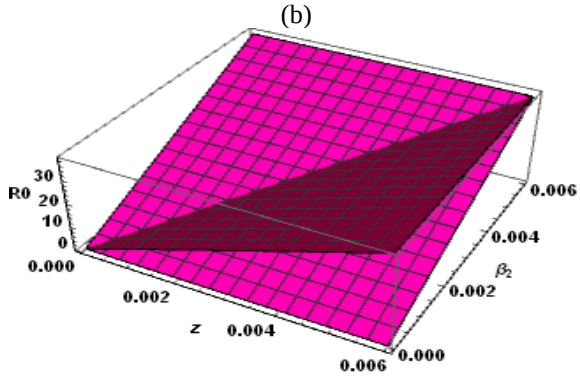

(c)

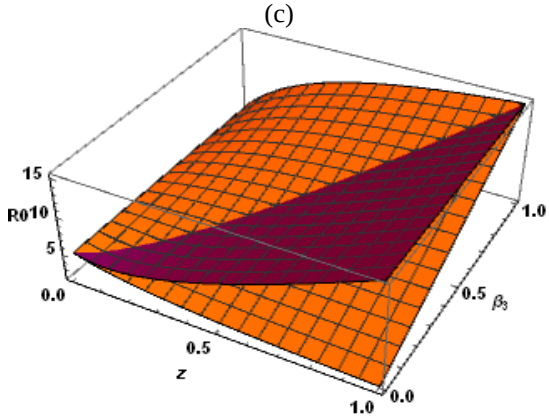

(d)

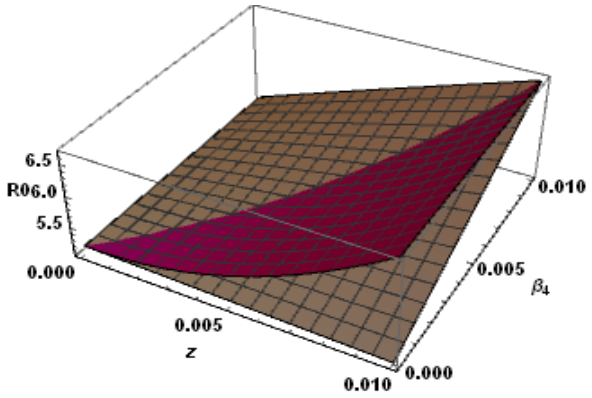

(e)

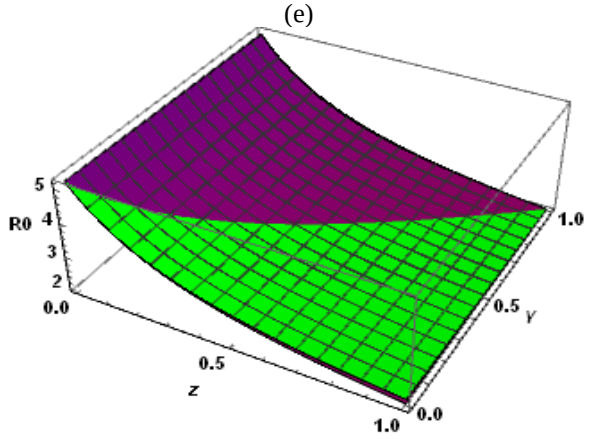

(f)

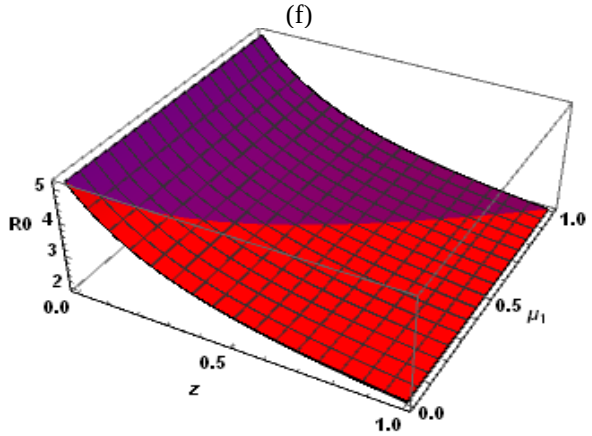

(g)

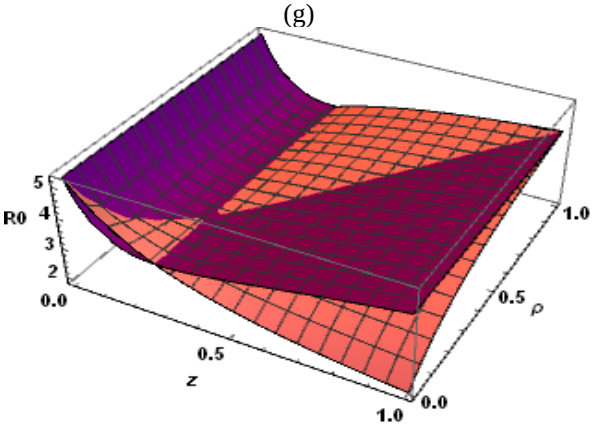

(h)

Figure 8. The dynamics of sensitivity analysis with respect to parameters (a) z and A with R_0, (b) z and β_1 with R_0, (c) z and β_2 with R_0, (d) z and β_3 with R_0, (e) z and β_4 with R_0, (f) z and γ with R_0, (g) z and μ_1 with R_0 and (h) z and ρ with R_0

On the other hand, by increasing the value of z, γ, μ_1 decreases the chance of the population to be infected with HFMD, which was described in Figure 6 (f) and Figure 7 (a), (b). So, from this we conclude that by increasing these parameters decreases the basic reproduction number i.e., these parameters are inversely proportional to basic reproduction number R_0. Also, in Figures 8 and 9, we have described graphically about the dynamics of sensitivity analysis of various parameters such as z and γ respectively. Similarly, we can do simulation for other parameters.

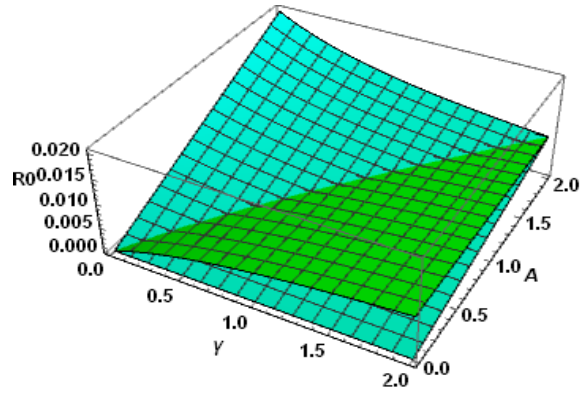

(a)

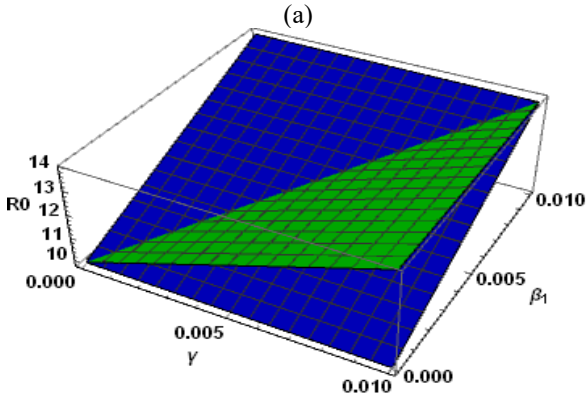

(b)

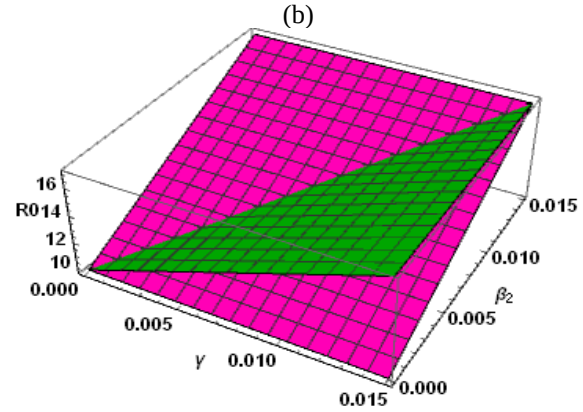

(c)

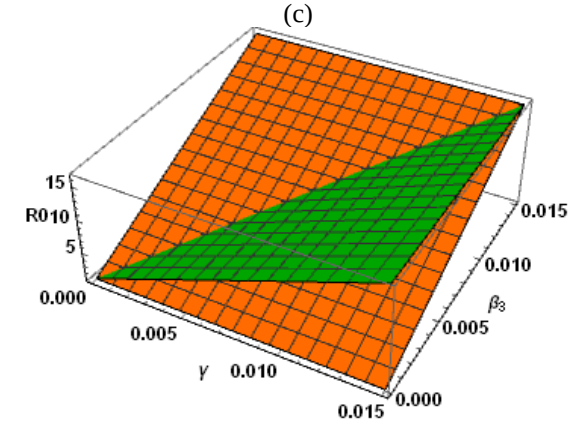

(d)

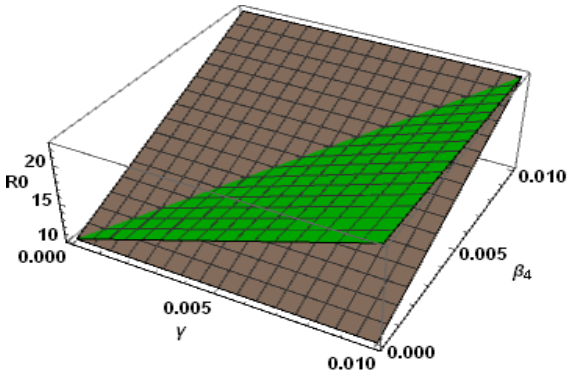

(e)

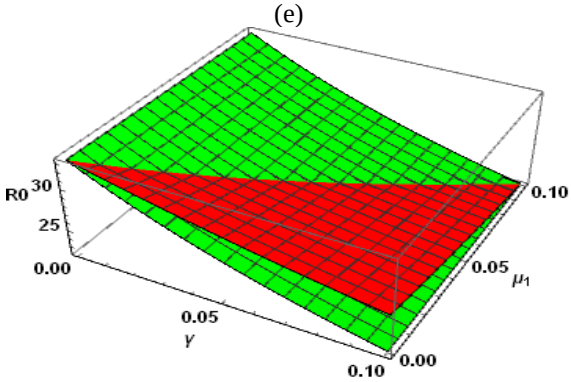

(f)

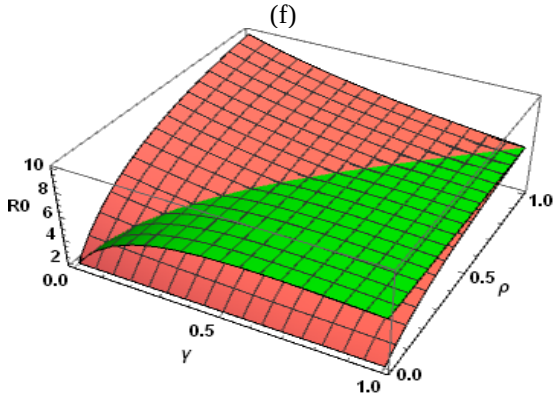

(g)

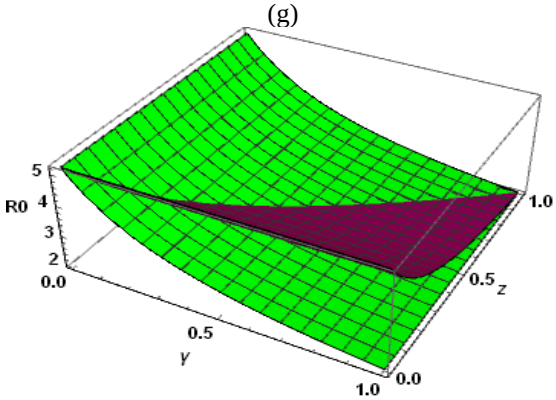

(h)

Figure 9. The dynamics of sensitivity analysis with respect to parameters (a) γ and A with R_0, (b) γ and β_1 with R_0, (c) γ and β_2 with R_0, (d) γ and β_3 with R_0, (e) γ and β_4 with R_0, (f) γ and z with R_0, (g) γ and μ_1 with R_0 and (h) γ and ρ with R_0

7. CONCLUSION

In our study, we focused on an HFMD compartmental model, structured to represent the susceptible, vaccinated, exposed, infected, and recovered human populations. The primary innovation of our work lies in the integration of a vaccinated class into the model's architecture. Our mathematical insights are chiefly derived from the formulation outlined in the proposed system (1). We initiated our analysis by establishing, positivity and boundedness of the system (1). Subsequently, we conducted an equilibrium analysis, identifying both the disease-free equilibrium (DFE) and the endemic equilibrium (EE) points within our system. A pivotal aspect of our investigation was the demonstration of the local asymptotic stability of the DFE when the basic reproduction number R_0 is less than one, and the local asymptotic stability of the EE when R_0 exceeds one. These stability assertions were rigorously established using the Jacobian matrix method. These insights are visually depicted in Figures 4(a), 4(b), 5(a), and 5(b), where the local stability of the disease-free state for $R_0 < 1$ and the endemic equilibrium for $R_0 > 1$ are clearly illustrated. Our exploration of global stability further enriched our analysis. Through the construction of a Lyapunov function, we established the global asymptotic stability of the DFE when $R_0 < 1$. Furthermore, we demonstrated the global asymptotic stability of the EE within the region Ω, leveraging Dulac's criteria. Moreover, we delved into the sensitivity analysis of the basic reproduction number R_0 systematically examining its variations across diverse parameters. Here, we observe that the parameters z and γ decreases the R_0. Also, we discussed about the dynamics of sensitivity analysis for z and γ parameters in Figure 8 and 9. The numerical results presented in this study provide a comprehensive overview of the HFMD model's behaviour across key parameters. So, by increasing the rate of vaccination z would probably reduce the risk of infection. This led us to control the HFMD transmission. These insights contribute significantly to our understanding of the intricate dynamics inherent in the spread of HFMD. This work can be extended and can be converted into fractional order model. Since, the fractional order models have become increasingly more important due to their ability to accurately describe intricate systems and phenomena that cannot be fully explained using traditional integer-order models. They provide a valuable tool set for understanding complex behaviour across a wide range of scientific and engineering disciplines.

REFERENCES

[1] Suvankar, M., Soovoojeet, J., Dhiraj Kumar, D., Kar, T.K. (2022). Global dynamics of a fractional-order HFMD model incorporating optimal treatment and stochastic stability. Chaos, Solitons and Fractals, 161: 112291. https://doi.org/10.1016/j.chaos.2022.112291

[2] Napasool, W., Ming Tang, I., Marc-Antoine, D., Puntani, P. (2021). Mathematical modeling and optimal control of the hand foot mouth disease affected by regional residency in Thailand. Mathematics, 9(22): 2863. https://doi.org/10.3390/math9222863

[3] Samanta, G.P. (2014). Analysis of a delayed hand-foot-mounth disease epidemic model with pulse vaccination. Systems Science Control Engineering, 2(1): 61-73. https://doi.org/10.1080/21642583.2014.880827

[4] Liu, J. (2011). Treshold dynamics for a HFMD epidemic model with periodic transmission rate. Nonlinear Dynamics, 64: 89-95. https://doi.org/10.1007/s11071-010-9848-6

[5] Tseng, F.C., Huang, H.C., Chi, C.Y., Lin, T.L., Liu, C.C., Jian, J.W., Hsu, L.C., Wu, H.S., Yang, J.Y., Chang, Y.W., Wang, H.C., Hsu, Y.W., Su, I.J., Wang, J.R. (2007). Epidemiological survey of enterovirus infections occurring in Taiwan between 2000 and 2005: Analysis of sentinel physician surveillance data. Journal of Medical Virology, 79(12): 1850-1860. https://doi.org/10.1002/jmv.21006

[6] https://www.thehindu.com/brandhub/hand-foot-and-mouth-disease/article65592261.ece.

[7] Schmidt, N.J., Lennette, E.H., Ho, H.H. (1974). An apparently new enterovirus isolated from patients with disease of the central nervouus system. The Journal of Infectious Diseases, 129(3): 304-309. https://doi.org/10.1093/infdis/129.3.304

[8] Repass, G.L., Palmer, W.C., Stancampiano, F.F. (2014). Hand, foot and mouth disease: identifying and managing an acute viral syndrome. Cleveland Clinic Journal of Medicine, 81(9): 537-543. https://doi.org/10.3949/ccjm.81a.13132

[9] Cabrerizo, M., Tarrago, D., Munoz-Almagro, C., Del, A.E., Domınguez-Gil, M., Eiros, J.M., Lopez-Miragaya, I., Perez, C., Reina, J., Otero, A. (2014). Molecular epidemiology of enterovirus 71, coxsackievirus A16 and A6 associated with hand, foot and mouth disease in Spain. Clinical Microbiology Infection, 20(3): 150-156. https://doi.org/10.1111/1469-0691.12361

[10] How, O.M., Chang, W.S., Anand, M., Yuwana, P., David, P., Daniella, C., Sylvia, D.S., Hee, C.C., Hooi, T.P., Jane, C.M. (2009). Identification and validation of clinical predictors for the risk of neurological involvement in children with hand, foot, and mouth disease in Sarawak. BMC Infectious Diseases, 9: 3. https://doi.org/10.1186/1471-2334-9-3

[11] Aakash, M., Gunasundari, C. (2023). Effect of partially and fully vaccinated individuals in some regions of India: A mathematical study on COVID-19 outbreak. Communications in Mathematical Biology and Neuroscience, 2023: 25. https://doi.org/10.28919/cmbn/7825

[12] Sharmila, N.B., Gunasundari, C. (2022). Travelling wave solutions for a diffusive prey-predator model with one predator and two preys. International Journal of Applied Mathematics, 35(5). https://doi.org/10.12732/ijam.v35i5.3

[13] Santhosh Kumar, G., Gunasundari, C. (2022). Turing instability of a diffusive predator - Prey model along with an allee effect on a predator. Communications in Mathematical Biology and Neuroscience, 2022: 40. https://doi.org/10.28919/cmbn/7361

[14] Aakash, M., Gunasundari, C., Al-Mdallal, Q.M. (2023). Mathematical modeling and simulation of SEIR model for COVID-19 outbreak: A case study of Trivandrum. Frontiers in Applied Mathematics and Statistics, 9. https://doi.org/10.3389/fams.2023.1124897

[15] Sharmila, N.B., Gunasundari, C. (2023). Mathematical Analysis of prey predator models with Holling type I functional responses and time delay. Communications in Mathematical Biology and Neuroscience, 2023: 72. https://doi.org/10.28919/cmbn/8014

[16] Wang, Y.C., Sung, F.C. (2007). Modelling the infectious for entero viruses in Taiwan. Institute of Environmental Health, China Medical University College of Public Health.

[17] Chen, S., Yang, D., Liu, R., Zhao, J., Yang, K., Chen, T. (2019). Estimating the transmissibility of hand, foot, and mouth disease by a dynamic model. Public Health, 174: 42-48. https://doi.org/10.1016/j.puhe.2019.05.032

[18] Phonchan, P., Naowarat, S. (2019). Sensitivity analysis of hand foot mouth disease model with public health resources. Southeast Asian. Journal of Sciences, 7(1): 59-70.

[19] Huang, Z., Wang, M., Qiu, L., Wang, N., Zhao, Z., Rui, J., Wang, Y., Liu, X., Hannah, M.N., Zhao, B., Su, Y., Zhao, B., Chen, T. (2019). Seasonality of the transmissibility of hand, foot and mouth disease: A modelling study in Xiamen City, China. Epidemiology and Infection, 147: E327. https://doi.org/10.1017/S0950268819002139

[20] Shi, L., Zhao, H., Wu, D. (2018). Modelling and analysis of HFMD with the effects of vaccination, contaminated environments and quarantine in mainland China. Mathematical Biosciences and Engineering, 16(1): 474-500. https://doi.org/10.3934/mbe.2019022